Journal of Applied Polymer Science

Smoke and toxicity suppression by zinc salts in flame-retardant polyurethane-polyisocyanurate foams filled with phosphonate and chlorinated phosphate

Xiu Liu, You Zhou, Jianwei Hao, Jianxin Du

National Laboratory of Flame Retardant Materials, National Engineering and Technology Research Center of Flame Retardant Materials, School of Materials Science and Engineering, Beijing Institute of Technology, Beijing 100081, People's Republic of China

Correspondence to: J. Hao (E-mail: hjw@bit.edu.cn)

ABSTRACT: Three types of zinc salts, $ZnAl_2O_4$, $ZnFe_2O_4$, and Zn_2SiO_4, were prepared by coprecipitation. Potential smoke and toxicity suppression by zinc salts in flame-retardant polyurethane-polyisocyanurate foams (FPUR-PIR) with dimethylmethylphosphonate (DMMP) and tris (2-chloropropyl) phosphate (TCPP) were investigated. The crystal structure and dispersity of zinc salts in FPUR-PIR were characterized by X-ray diffraction (XRD) and scanning electron microscopy (SEM). Smoke density, flame retardancy, and thermal degradation were studied using smoke density rating (SDR), limiting oxygen index (LOI), the cone calorimeter test, and thermogravimetry coupled with FTIR spectrophotometry (TGA-FTIR). The results indicated that pure zinc salts were obtained and evenly dispersed on the cell wall of FPUR-PIR. SDR and the specific extinction area (SEA) were significantly decreased, the time to second heat release rate peak (pk-HRR) of FRUP-PIR was delayed after incorporation of the zinc salts; zinc salts partially inhibited phosphorus oxide release into the gas phase, enhanced the condensed phase effect of phosphorus, reduced, and prolonged the release of isocyanate compound and hydrogen cyanide from FRUP-PIR; due to an increase in the amount of char residues, which indicated the suppression of smoke and toxicity volatiles. $ZnFe_2O_4$ resulted in better char formation at the initial degradation stage of FPUR-PIR, and $ZnAl_2O_4$ retained more phosphorus in the solid phase at higher temperature. © 2014 Wiley Periodicals, Inc. J. Appl. Polym. Sci. **2015**, *132*, 41846.

KEYWORDS: addition polymerization; flame retardance; foams; polyurethanes; thermal properties

Received 29 July 2014; accepted 6 December 2014

DOI: 10.1002/app.41846

INTRODUCTION

In recent years, more attention has been paid to the smoke density and toxicity of insulation materials. Increasing awareness of the fire safety of materials has led to the approval of new regulations,[1] where smoke density and toxicity are very important factors and should be considered in the evaluation of fire safety.

Polyurethane foam is considered to be an ideal alternative to inorganic insulation materials in buildings and insulated appliances.[2] However, polyurethane foams readily ignite and burn rapidly with a high rate of heat release and evolution of smoke and toxic gases such as carbon monoxide and hydrogen cyanide.[3,4] To reduce the flammability of polyurethane foam, liquid halogenated phosphates such as tris (2-chloropropyl) phosphate (TCPP), and phosphonates such as dimethylmethylphosphonate (DMMP) and phosphonate derivatives as flame retardants are widely used due to their excellent flame retardancy, economy, and suitability for spraying. Phosphonate and chlorinated phosphate can not only form phosphoric anhydrides and related acids which act as dehydrating agents to promote char formation, but also release phosphorus containing radicals which inhibit flames through a radical trapping mechanism in the gas-phase to reduce the flame energy[5] of flame-retardant polyurethane foams in combustion.

However, phosphonate and chlorinated phosphate evolved abundant phosphorus oxides and degradation fragments during combustion. Furthermore, the lower thermal degradation temperatures of these phosphonates and acid catalysis to polyurethane enable a decrease in the onset thermal degradation temperatures of materials which leads to the premature release of degradation fragments. These factors further significantly increase smoke density and toxicity,[5,6] which is not conducive for fire rescue. Thus, a smoke suppression study on polyurethane with phosphonate and chlorinated phosphate is necessary.

To decrease the smoke density and toxicity of degradation products of polymers during combustion, metal compounds have

been extensively studied due to their smoke suppression in various polymers. Metal oxides[7,8] and metal salts[9] as smoke suppressants have good performance in polymers. It has also been observed that metal compounds as Friedel-Crafts catalysts may promote the crosslinking of polystyrene in some cases.[10] Dhakate[11] and Weil[12] reported that metal compounds may have graphitization and crosslinking activities. In addition, metal compounds promote the crosslinking of phosphorus flame retardants,[13,14] promote phosphorus retention in the solid phase, and reduce the evolution of phosphorus oxides during combustion.[15]

Some studies[9,16] reported that a mixture of different metal compounds had good synergistic effects on flame retardancy and smoke suppression. Some metal salts such as zinc stannate and zinc aluminate have been used in polymers as smoke suppressants.[17,18] Su *et al.*[19] reported that Zn^{2+} can promote dehydrogenation and esterification, and the presence of SnO_3^{2-} can accelerate the crosslinking process of polyphosphoric acid and pentaerythrite, the synergistic effect makes the residue char more stable at higher temperature. Furthermore, good contact and the synergism between different atoms in this type of compound may result in excellent smoke suppression in polymers. Thus, the potential effect of composite metal salt compounds in the thermal degradation process of polymers should be investigated.

In this study, composite metal compounds, $ZnAl_2O_4$, $ZnFe_2O_4$, and Zn_2SiO_4, as smoke suppressants were prepared by coprecipitation. The potential smoke and toxicity suppression and flame retardancy effects of these zinc salts in flame-retardant polyurethane-polyisocyanurate (FPUR-PIR) foams with dimethylmethyl phosphonate (DMMP), and tris (2-chloropropyl) phosphate (TCPP) were investigated. The thermal degradation behaviors of FPUR-PIR-added zinc salts were studied by TG-FTIR.

EXPERIMENTAL

Raw Materials

The materials used to prepare zinc salts were $NaAlO_2$, $Zn(NO_3)_2{\cdot}6H_2O$, $Fe(NO_3)_3{\cdot}H_2O$, Na_2SiO_3, $ZnSO_4$, NaOH, all were analytical grade and purchased from Tianjin Kemao Chemical of China. Polyester polyol (4110A, functionality, 3.0; hydroxyl value, 410–460 mg KOH/g; viscosity at 25°C, 4500 mPa s), polyaryl polymethylene isocyanate (PAPI, NCO %, 30.5; average functionality, 2.8; viscosity at 25°C, 600 mPa s) were all purchased from BASF. The catalyst employed for cyclotrimerisation of isocyanate was 401 (Main component is pentamethyldiethylentriamine), provided by Shanghai Chemical Reagent Co (Shanghai, China). A silicon-based surfactant NIAX silicon SR-393 as surfactant agent was purchased from Shanghai Chemical Reagent (Shanghai, China). Blowing agent, n-pentane (technical grade) was provided by Shanghai Chemical Reagent of China. Flame retardants, dimethylmethylphosphonate (DMMP) and tris (2-chloropropyl) phosphate (TCPP) were supplied by Jacques Jiangsu Science and Technology of China.

Preparation of Zinc Salts

Preparation of $ZnAl_2O_4$. $NaAlO_2$ and $Zn(NO_3)_2{\cdot}6H_2O$ (2 : 1 mol/mol) were dissolved in stirred distilled water, followed by the addition of drops of 0.1*M* aqueous NaOH to reach a pH of 11–12, and stirred for 30 min. After 24 h, the precipitate was filtered, underwent calcination for 4–5 h at 700°C, and the product, ZA, was obtained.

Preparation of $ZnFe_2O_4$. $Zn(NO_3)_2{\cdot}6H_2O$ and $Fe(NO_3)_3{\cdot}H_2O$ (1 : 2 mol/mol) were dissolved in stirred distilled water, followed by the addition of drops of 0.1*M* aqueous NaOH to reach a pH of 12, stirred for 30 min, heated to 100°C, refluxed for 2 h, filtered after cooling, underwent calcination for 2 h at 600°C, and the product, ZF, was obtained.

Preparation of Zn_2SiO_4. Na_2SiO_3 was dissolved in distilled water, followed by the addition of drops of $ZnSO_4$ solution (molar ratio of Na_2SiO_3 to $ZnSO_4$ was 2 : 1), stirred for 30 min, heated to 100°C, refluxed for 6 h, filtered after cooling, underwent calcination for 4 h at 700°C, and the product, ZS, was obtained.

Preparation of Foam Composites

A one-shot, free-rise method was used to prepare neat FPUR-PIR using a cast mold. Polyol, flame retardants, and zinc salts were mixed and stirred with an electric stirrer until a uniform mixture was obtained. Isocyanate was then quickly added to the suspension. After high speed stirring at 1500 rpm for about 10 s, the mixture was poured quickly into the cast mold. The mixture was allowed to foam at room temperature and the foam was placed in an oven and heated for 2 h at 60°C. The foam was then taken out of the mold. Test samples with their coats removed were machined in accordance with the test standard.

In this study, the molar ratio of NCO to OH was 2.5; the weight ratio of polyol to isocyanate was 100 : 209. TCPP, DMMP and zinc salts content was fixed at 20 g:10 g:6 g per 100 g of polyols. The FPUR-PIR foams filled with ZA, ZS, and ZF were abbreviated to FPUR-PIR-ZA, FPUR-PIR-ZS, and FPUR-PIR-ZF, respectively.

Characterization

X-ray Diffraction. X-ray diffraction (XRD) measurement was performed using a Bruker-AXS diffractometer equipped with a Cu anode X-ray tube and diffracted beam monochromator (40 Kv, 30 Ma, λ Cu Kα = 0.1542 nm). Zinc salts were scanned in an angle range from 20 to 80°.

Scanning Electron Microscopy and Energy Dispersive Spectrometer. FPUR-PIR samples were fractured at room temperature and coated with gold before being investigated under a scanning electron microscope. The fracture surfaces of the samples were observed with a S-4800 (JEOL Japan) SEM with an accelerating voltage of 5 kV.

Transmission Electron Microscopy. TEM micrographs were obtained using a JEOL 2100 with an acceleration voltage of 200 kV.

Smoke Density Rating. The SDR was determined with a JCY-2 instrument (Nanjing Analysis Instrument Factory, China) according to the ASTM D2843 method; the size of the test specimens was 25.4 × 25.4 × 6.0 mm^3.

Limited Oxygen Index Test. LOI was measured on an FTA-II instrument (Rheometric Scientific) with the specimen dimensions of 130 × 10 × 10 mm^3, according to ASTM D 2863-97.

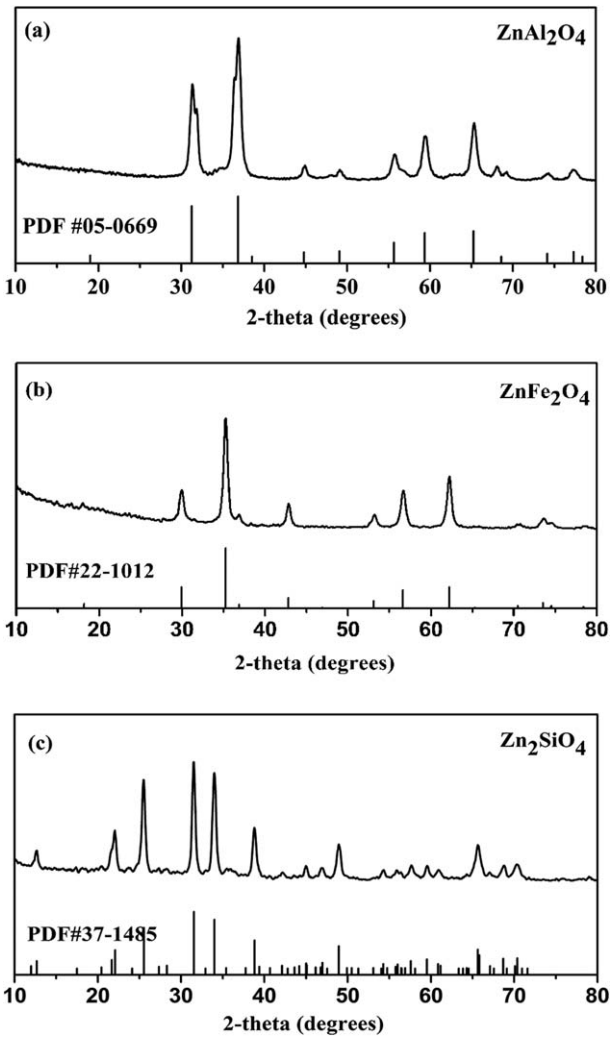

Figure 1. XRD patterns of ZA (a), ZF (b), and ZS (c).

Cone Calorimetry. Cone calorimeter measurements were performed at an incident radiant flux of 45 kW m^{-2}, according to ISO 5660 protocol, using a fire Testing Technology apparatus with a truncated cone-shaped radiator. The specimen (100 × 100 × 30 mm^3) was measured horizontally without any grids. Parameters such as heat release rate (HRR), peak heat release rate (pk-HRR), average specific extinction area (av-SEA), total smoke production (TSP), total smoke released (TSR), total heat released (THR), remaining residue are recorded within the time of 450 s after tests started.

Thermogravimetric Analysis-Fourier Transform Infrared Spectroscopy. Thermogravimetric Analysis-Fourier Transform Infrared Spectroscopy (TGA-FTIR) measurement was carried out on a Netzsch TG 209 F1 thermogravimeter coupled with a Nicolet 6700 FTIR spectrophotometer. About 4 mg of each sample was heated from 50°C to 800°C with a heating rate of 20°C/min under nitrogen (flow rate = 20 mL min^{-1}). The couple system between TGA and FTIR was a quartz capillary kept at temperature of 200°C. Pyrolysis gases from the samples in the thermogravimetric analyzer were blown to the FTIR spectrometer with the guide by nitrogen. About 32 scans within the range of 4000–400 cm^{-1} were done for each sample with a resolution of 4 cm^{-1}.

The apparent density of the foam samples were measured according to ASTM D 1622-03. The size of the specimen was 30 × 30 × 30 mm^3. The apparent densities of five specimens per sample were measured, and then the average values were reported.

RESULTS AND DISCUSSION

Structure and Dispersion

The crystal structure and dispersity of zinc salts in FPUR-PIR were characterized by XRD, TEM, and SEM, and the results are shown in Figures 1–4, respectively. It can be seen that target products were obtained. The diffraction peaks of ZA, ZF, and ZS (Powder Diffraction File cards: 05–0669, 22–1012, 37–1485) are presented in Figure 1.

Figure 2 shows the TEM micrographs of the zinc salts, and it can be seen that the particle size of the zinc salts are almost in the tens of nanometers. Figures 3 and 4 show the SEM micrographs and EDS (Energy Dispersive Spectrometry) mapping images of the polyurethane–polyisocyanurate foams (PUR-PIR), and FPUR-PIR filled with zinc salts. The SEM micrographs of

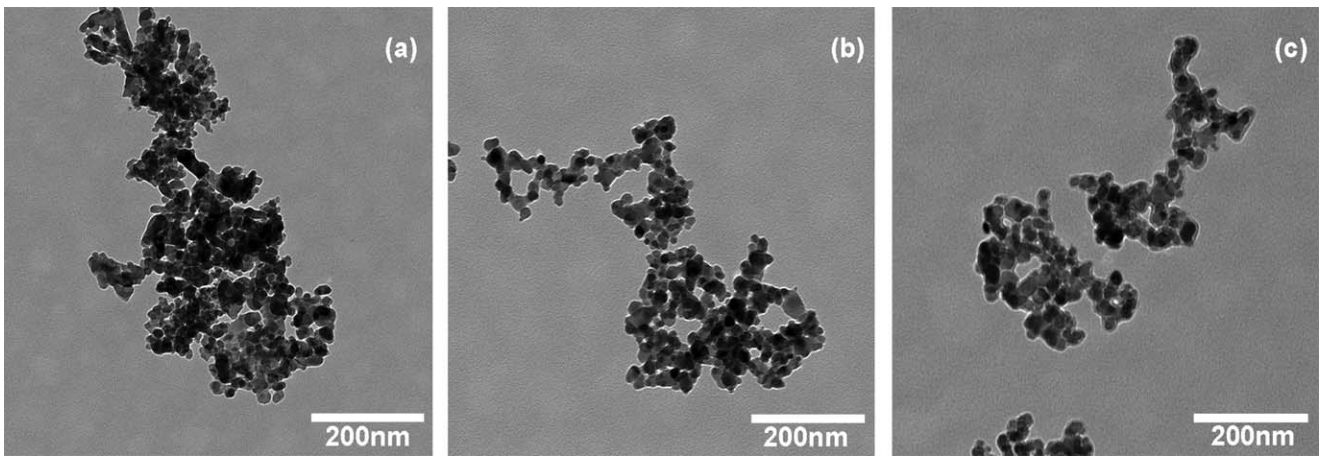

Figure 2. TEM micrographs of ZA (a), ZF (b), and ZS (c).

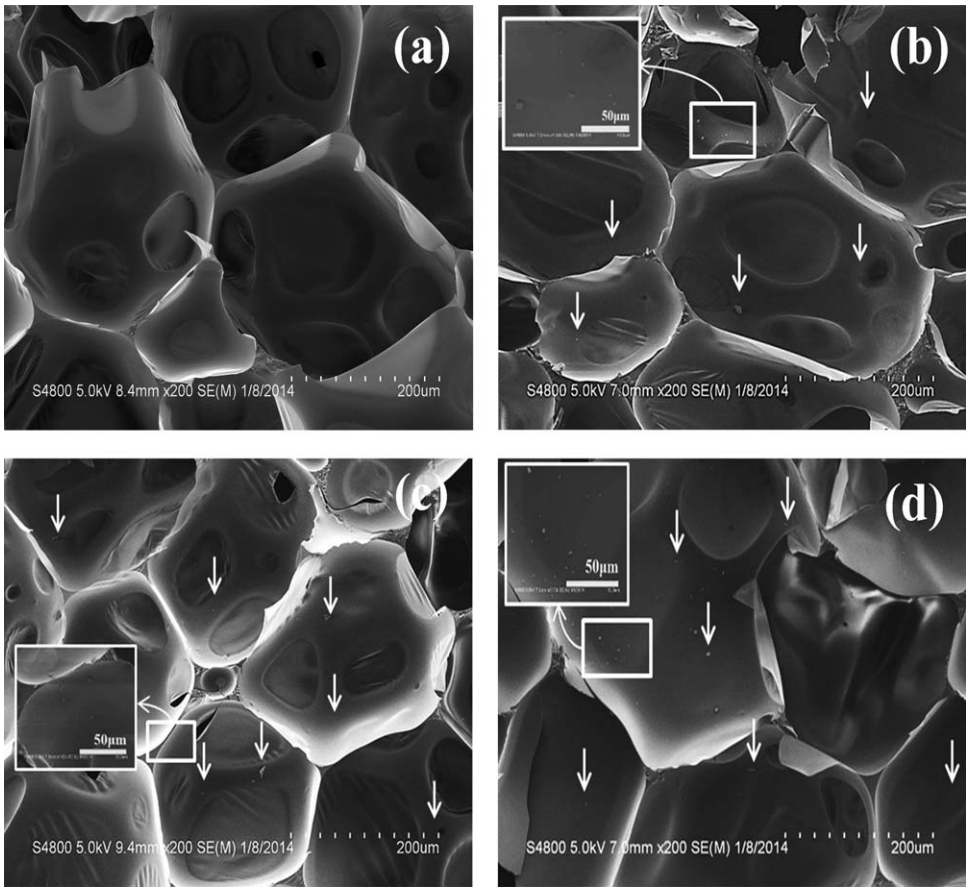

Figure 3. SEM micrographs of the PUR-PIR (a) and FPUR-PIR filled with ZA (b), ZF(c), and ZS (d).

PUR-PIR and FPUR-PIR filled with zinc salts are very similar. Thus, we have provided the SEM of PUR-PIR in Figure 3(a). From the magnified image insert in Figure 3, it can be seen that the zinc salts were well dispersed in the polymer matrix. Figure 4 shows the distribution of different elements (C, P, Zn) which shows that the phosphonate and zinc salts are uniformly distributed in the matrix. The shape of the cells of FPUR-PIR with zinc salts was regular, with no collapse or collision morphology observed. Due to the agglomeration of nanoparticles, particle sizes of the zinc salts on the cell wall were less than 10 μm.

Fire and Smoke Behavior

Smoke Density and LOI. To estimate the smoke suppression and flame retardancy of zinc salts in FPUR-PIR, the SDR and LOI tests were performed. Density values, SDR and LOI of PUR-PIR, FPUR-PIR, and FPUR-PIR with zinc salts are presented in Table I. It can be seen that the zinc salts slightly increased the density of FPUR-PIR. The addition of DMMP and TCPP resulted in an increase in the smoke density of PUR-PIR, zinc salts significantly decreased the SDR of FPUR-PIR, and LOI was slightly changed in all samples. In order to reduce the impact of the density difference on SDR test results, SDRpm (smoke density rating of unit mass sample) was defined. FPUR-PIR-filled zinc salts had lower SDRpm compared with FPUR-PIR. The greatest decrease (43.9%) in SDRpm and greatest increase in LOI were obtained by FPUR-PIR-ZA. The decrease in SDRpm indicated that the three types of zinc salts had a smoke reducing effect.

Smoke and Heat Release. The smoke and heat release behaviors of PUR-PIR, FPUR-PIR, and FPUR-PIR filled with zinc salts were quantitatively evaluated by cone calorimetry. A cone calorimeter is an effective bench scale apparatus which simulates real fire scenarios. Detailed data from cone calorimetry are reported in Table II and Figure 5. It can be seen that phosphonates decreased the pk-HRR of PUR-PIR, and significantly increased the av-SEA and CO production; pk-HRR, av-SEA, TSR, TSP, and CO production from FPUR-PIR filled with zinc salts were much lower than those from FPUR-PIR. From Figure 5(c), it can be seen that ZA significantly decreased the COP value. Moreover, compared with FPUR-PIR, THR was increased, average residual mass was enhanced by 3–7 wt %; the time to second pk-HRR was delayed by approximately 30 s for FPUR-PIR filled with zinc salts.

The THR for FPUR-PIR filled with zinc salts was slightly increased compared to FPUR-PIR, this also indicated that the flame inhibition by phosphorus was diminished in the gas phase due to competitive reactions that promote retention of phosphorus in the solid phase.[15] In addition, ZS decreased TSR and TSP, and delayed the second pk-HRR of FPUR-PIR; however, FPUR-PIR-ZA performed better than FPUR-PIR-ZS in the SDR test, this was partly due to the intrinsic difference between ZA

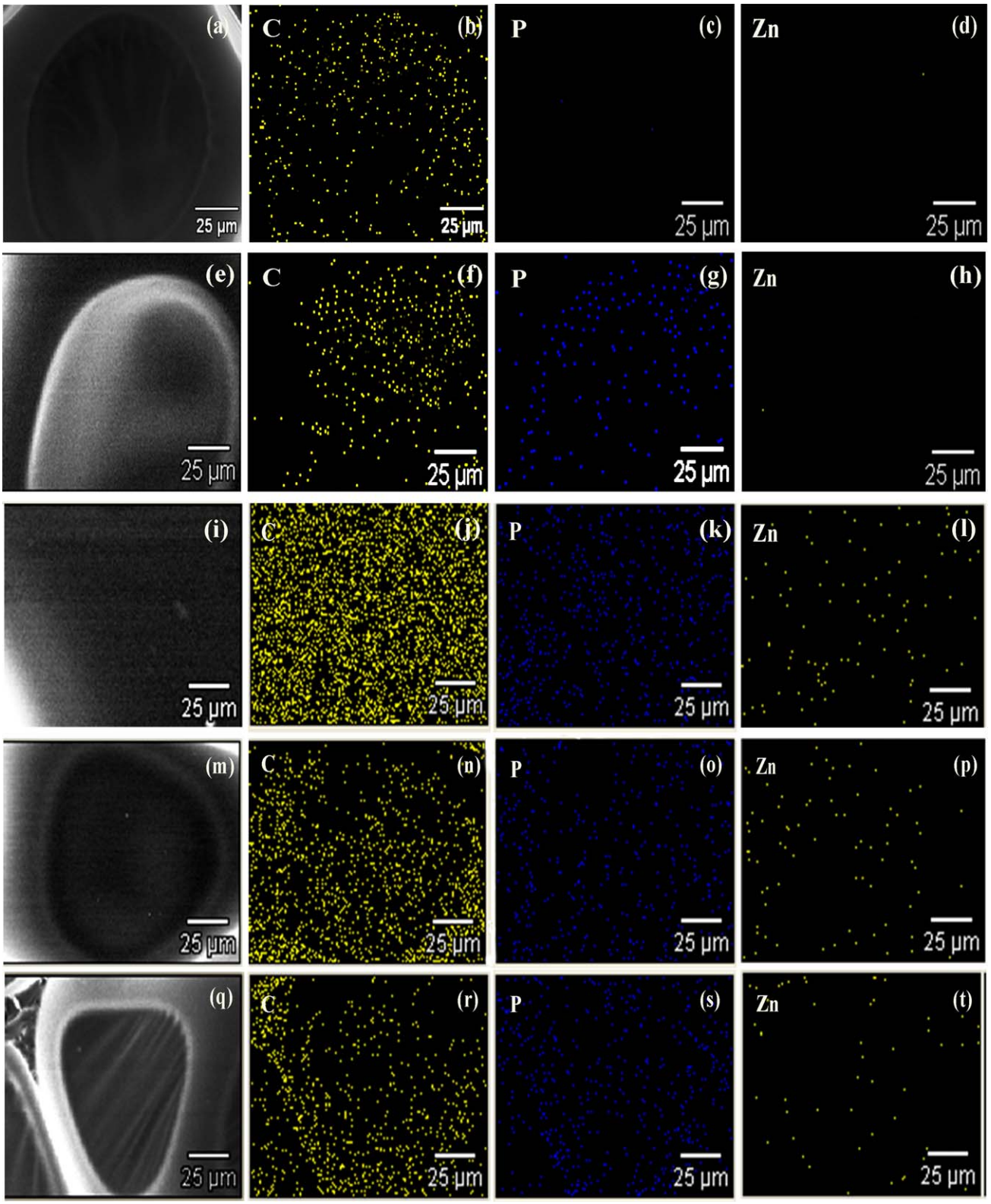

Figure 4. EDS mapping images of (a–d) PUR-PIR, (e–h) FPUR-PIR, FPUR-PIR filled with ZA (i–l), ZF (m–p), ZS (q–t). [Color figure can be viewed in the online issue, which is available at wileyonlinelibrary.com.]

and ZS, and the difference between the two test methods. The differences in the tests lead to inconsistencies in test results.[15] The SDR test involves small sized material and powerful flames under static conditions in a smoke box, and provides information on milligram samples. Cone calorimetry involves macro-sized material which burns quietly under thermal radiation in

Table I. LOI and SDR Tests Results of FPUR-PIR and FPUR-PIR Filled with Zinc Salts

Sample	SDR	SDR_{pm}[a] (g^{-1})	SDR_{pm} reduction[b] (%)	Density (kg m^{-3})	LOI (%)
PUR-PIR	21.6 ± 0.5	112.8 ± 3.1	-	43.7	21.0
FPUR-PIR	30.6 ± 1.4	185.9 ± 5.1	-	46.7	26.2
FPUR-PIR-ZA	20.8 ± 1.2	104.2 ± 6.9	43.9	50.0	26.5
FPUR-PIR-ZF	29.1 ± 0.2	148.5 ± 0.9	20.1	51.7	26.0
FPUR-PIR-ZS	23.6 ± 1.3	122.5 ± 1.3	34.1	47.5	26.3

[a] SDR_{pm} is SDR of unit mass sample.
[b] SDR_{pm} reduction is the decrease percent of SDR_{pm} compared with FPUR-PIR.

circulating air, and provides information on samples of several tens of grams.

Thermal and Toxicity Behavior

TGA. Based on the above combustion tests, in order to track the different processes of weight loss and charring between FPUR-PIR and FPUR-PIR filled with zinc salts, the thermal behavior of the samples under an inert atmosphere was observed by TGA, and the results are shown in Figure 6 and Table III. PUR-PIR, FPUR-PIR, and its composites exhibited three main degradation stages. After adding ZA, ZS, and ZF, the temperatures of the first and third degradation peaks were delayed by 2–5°C, their maximum mass loss rates all decreased, and the amount of char residue at 800°C increased by 1.3–3.1% compared with FPUR-PIR (Table III).

The resultant effects of zinc salts on FPUR-PIR can be explained as follows: DMMP and TCPP have lower initial degradation temperatures than the polymer matrix. When composites were heated to approximately 190°C, phosphonate degraded first.[20,21] The reduction in initial decomposition temperature was attributed to the fact that the P—O—C bond is less stable than the common C—C bond.[22,23] The temperatures of the first and third maximum mass loss rates of all FPUR-PIR filled with zinc salts were increased and the corresponding mass loss rates were decreased. This also explained the delay in the second PHRR in the cone calorimeter test.

It is worth noting that ZF was excellent in delaying the first thermal degradation peak temperature by about 15°C compared with FPUR-PIR. ZA was excellent not only in decreasing mass loss rate at the second degradation peak, but it also increased the char residue. This may be attributed to iron, which as a transition metal, has higher catalytic activity in char formation at the initial stage.[15] Therefore, the temperature of the first degradation peak of FPUR-PIR increased. The better performance of ZA at higher temperature may be attributed to the char being more stable at higher temperature.[9]

Toxicity Suppression. From the above data on thermal degradation of the composites, some macroscopic information was obtained. In order to further understand the way zinc salts inhibit the vapor retardant effect of phosphorus, reduce the release of smoke and toxic products, and retain more degradation fragments in the solid phase, TG-FTIR was employed to analyze the evolved gases from all formulations during thermal degradation.

The FTIR spectra of pyrolysis products of FPUR-PIR at its three weight loss peaks (190°C, 336°C and 447°C) are presented in Figure 7. Phosphorus oxides such as P═O (1280 cm^{-1}) and PO_2^- (1060 cm^{-1}) were detected during the first mass loss stage which can be attributed to the degradation of phosphonate and some small molecule compounds.[24] The second mass loss was due to degradation of the polymer chain and the third mass loss stage was due to the further degradation of the char residue which degradates only at higher temperatures. In these cases, many types of products were released such as CO, CO_2 (2352, 2310 cm^{-1}), —NHC═O (1528 cm^{-1}), C—O—C (1057 cm^{-1}) and others,[25–27] as shown in Table IV.

According to the above analysis, to understand the changes in these pyrolysis products and study the effects of zinc salts on phosphorus oxide release, the relationships between intensity of the characteristic peak and release time for volatilized PO_2^-, —NCO containing compounds and HCN are plotted in Figures 8 and 9, respectively. Figure 8 shows the FTIR spectra of PO_2^- (1060 cm^{-1}) for the gases produced from thermal degradation of all samples. It can be seen that the initial release time of PO_2^- from FPUR-PIR filled with zinc salts at about 7 min was delayed 1−2 min compared with FPUR-PIR. This is consistent with the delay in the first degradation peak in the TGA test.

Table II. Cone Calorimetric Data of PUR-PIR, FPUR-PIR, and FPUR-PIR Filled with Zinc Salts (Heat Flux of 45 kW m^{-2})

Sample	av-SEA(m^2 kg^{-1})	TSP (m^2 kg^{-1})	pk-HRR (kW m^{-2})	THR (MJ m^{-2})	Residual mass (%)
PUR-PIR	451.7 ± 21	5.5 ± 0.3	185.1 ± 0.5	31.5 ± 0.9	26.6
FPUR-PIR	831.2 ± 19	6.5 ± 0.5	112.2 ± 2.3	20.6 ± 0.7	24.8
FPUR-PIR-ZA	654.4 ± 6	6.0 ± 0.2	106.6 ± 1.2	22.9 ± 1.2	28.6
FPUR-PIR-ZF	475.6 ± 1	6.2 ± 0.1	110.0 ± 1.3	23.3 ± 1.0	27.9
FPUR-PIR-ZS	485.5 ± 7	5.6 ± 0.1	103.4 ± 0.8	22.6 ± 0.5	31.8

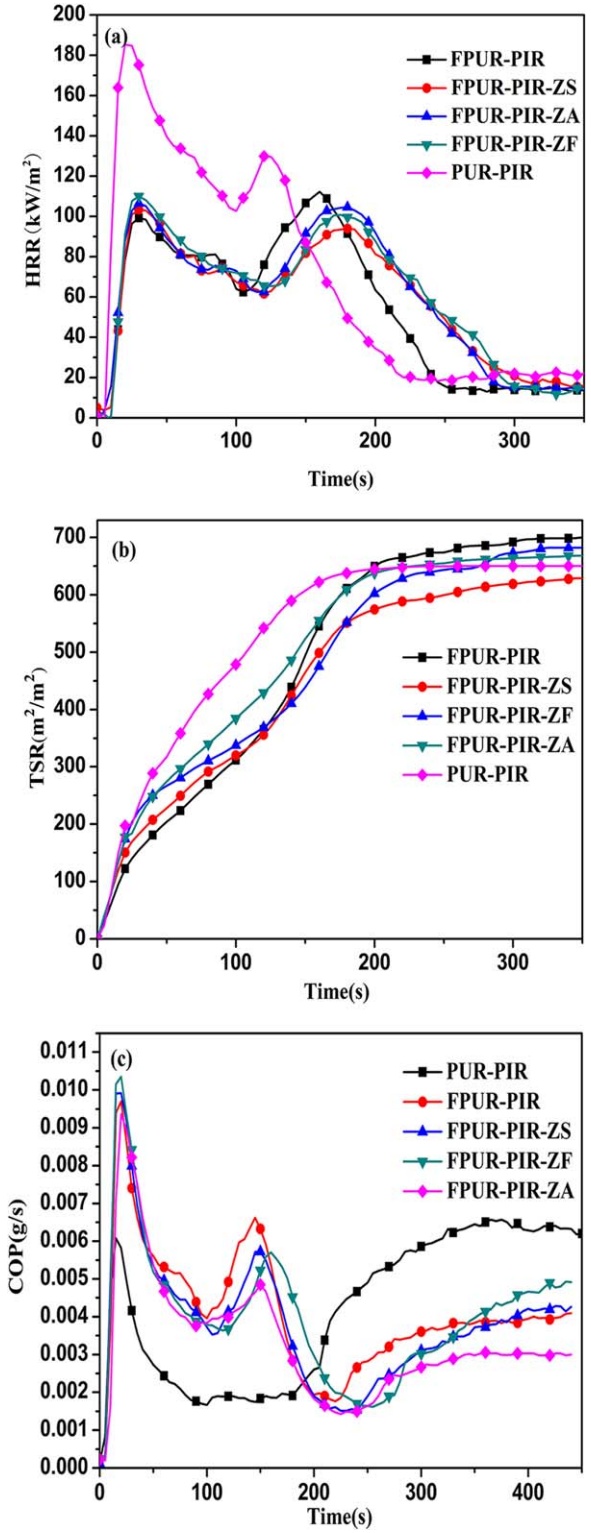

Figure 5. (a) HRR, (b) TSR and (c) CO production curves of PUR-PIR, FPUR-PIR, and FPUR-PIR filled with zinc salts (45 kW m^{-2}). [Color figure can be viewed in the online issue, which is available at wileyonlinelibrary.com.]

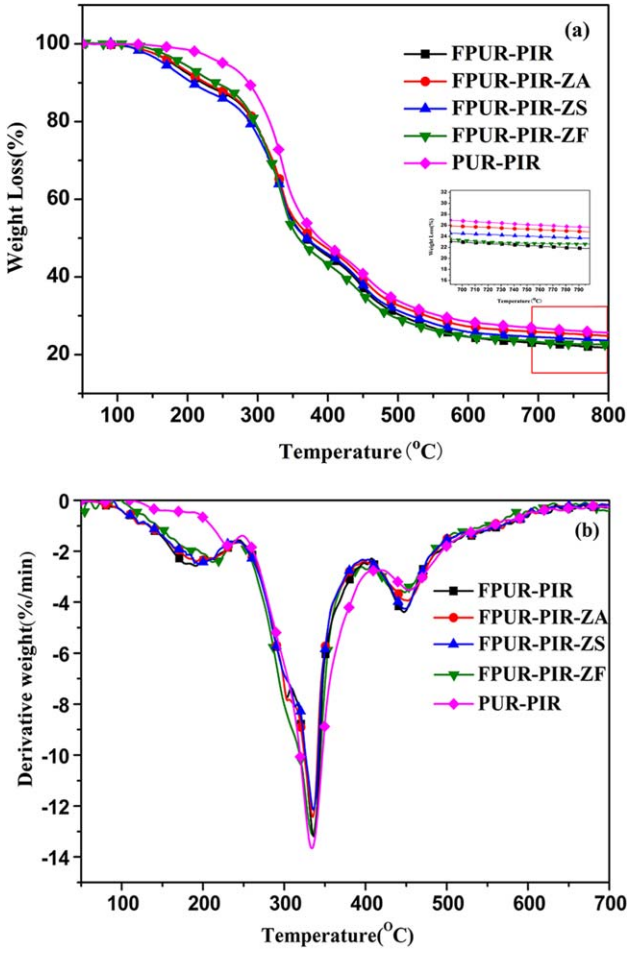

Figure 6. (a) TGA and (b) DTG curves of PUR-PIR, FPUR-PIR, and FPUR-PIR filled zinc salts under nitrogen. [Color figure can be viewed in the online issue, which is available at wileyonlinelibrary.com.]

The generated trends in —NCO (2275 cm^{-1}) are shown in Figure 9(a). It can be seen that the release of —NCO from PUR-PIR began at about the fifth minute and from FPUR-PIR at the sixth minute. The addition of zinc salts delayed the initial release time of —NCO to about the eighth minute. The –NCO absorption peak strength of FPUR-PIR filled with zinc salts at 8 min and 10−15 min were all lower than for PUR-PIR and FPUR-PIR.

Figure 9(b) shows the generated trend of HCN. Some studies have reported[5,28] that the evolution of HCN starts at 550°C, and the absorption peaks at 710−715 cm^{-1}. At low temperatures, the generation of HCN is negligible. The addition of zinc salts delayed and dispersed the release peak of HCN.

Because of the number of toxicity products affected by the mass of sample, the peak area per unit mass was calculated, and the ratio of peak area per unit of mass between FPUR-PIR filled with zinc salts and FPUR-PIR are shown in Table V. It can be seen that the addition of zinc salts decreased the number of toxic products released, ZF performed well in decrease the release of PO_2^- and HCN, and ZA performed well in decrease the release of —NCO. The decrease in HCN was mainly due to the metal atoms which catalyzed the conversion of nitrogen-containing compounds to nitrogen oxides (NO_x) at the initial HCN generating stage.[7] Relatively stable char inhibited the

Table III. TGA Data of PUR-PIR, FPUR-PIR, and FPUR-PIR Filled with Zinc Salts Under Nitrogen

	First peak		Second peak		Third peak		
Sample	Temp (°C)	Mass loss rate (%·min^{-1})	Temp (°C)	Mass loss rate (%·min^{-1})	Temp (°C)	Mass loss rate (%·min^{-1})	Char residue at 800°C (%)
PUR-PIR	231.4	1.8	334.1	13.7	453.7	3.5	24.9
FPUR-PIR	190.8	2.6	336.3	13.4	447.3	4.6	21.1
FPUR-PIR-ZA	191.6	2.4	336.1	12.3	451.8	4.0	24.2
FPUR-PIR-ZF	205.4	2.3	335.9	13.3	449.1	3.6	22.5
FPUR-PIR-ZS	192.0	2.4	336.2	12.2	448.6	4.5	23.3

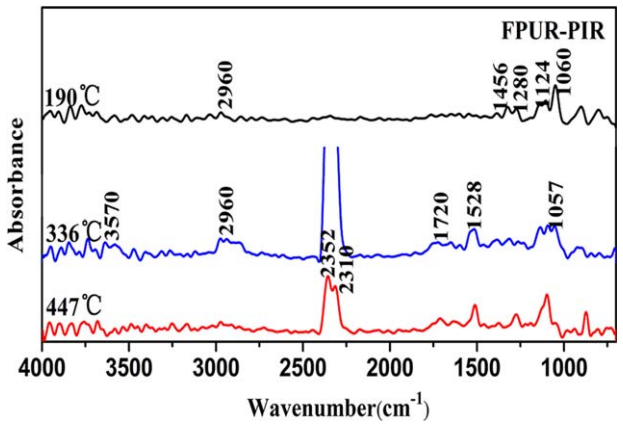

Figure 7. FTIR spectra of the pyrolysis products of FPUR-PIR at the maximum evolution rates. [Color figure can be viewed in the online issue, which is available at wileyonlinelibrary.com.]

release of nitrogen-containing compounds. In these cases, zinc salts effectively suppressed the release of smoke and toxic products.

Morphology and Chemical Composition of the Char Residues. In order to obtain more insight into the catalysis of zinc salts in char formation, the residues obtained during cone calorimetry were homogenized and analyzed by FTIR. Figure 10 shows the FTIR spectra of the solid residues. For PUR-PIR and FPUR-PIR, the FTIR spectra of residues were similar due to the almost complete degradation of PUR-PIR and phosphonate. With respect to FPUR-PIR, solid residues of FPUR-PIR filled with zinc salts showed peaks at 728 cm^{-1} and 1121 cm^{-1} which were attributed to metal phosphate.[24] All spectra of residues contained a strong peak at 1528 cm^{-1} and a weak peak at 3050 cm^{-1}, which were attributed to aromatic compounds. In addition, FPUR-PIR filled with zinc salts showed a strong peak at 803 cm^{-1} (attributed to P—O—C), and FPUR-PIR filled with ZA was stronger than the others at this peak. This indicated that zinc salts retain more phosphorus in the solid phase, and ZA was better at retaining phosphorus in the solid phase at higher temperature which was consistent with the results of the TGA and Cone tests.

To further understand the relationship between the microstructure of char and the flame retardancy of FPUR-PIR, digital photographs and SEM images of char residues after cone calorimetry were obtained (Figures 11 and 12). It can be seen that the char structure of PUR-PIR [Figure 11(a)] was loose as shown in Figure 12(a) which was due to insufficient char formation. The char residue of FPUR-PIR [Figure 11(b)] was not good. In contrast, for FPUR-PIR filled with zinc salts, black structures were seen on the surface of the char layer [Figure 11(c−e)]. The char layer with more compact structure is shown in Figure 12(c–e) which is in accordance with Figure 11. The compact black structure leaded to better flame retardancy of FPUR-PIR filled with zinc salts.

Table IV. Assignment of Some Main Absorbance Bands of Pyrolysis Products of FPUR-PIR in the FTIR Spectra

Wavenumber (cm^{-1})	Assignment
3740-3550	O—H stretching vibration of phenol or H_2O
3160-3057	C—H stretching vibration of aromatic rings
2960, 2930	C—H stretching vibration of —CH_3, —CH_2—
2352, 2310	C=O stretching vibration of CO_2, CO
1700-1740	C=O stretching vibration of aromatic polyurethane compounds
1520-1560	N—H stretching vibration of —NHCO—
1450-1470	—CH_2— deformation vibration and-CH_3 asymmetric deformation vibration
1250-1299	P=O stretching vibration
1124	P—H stretching vibration of phosphine
1060	—O—P—O— stretching vibration

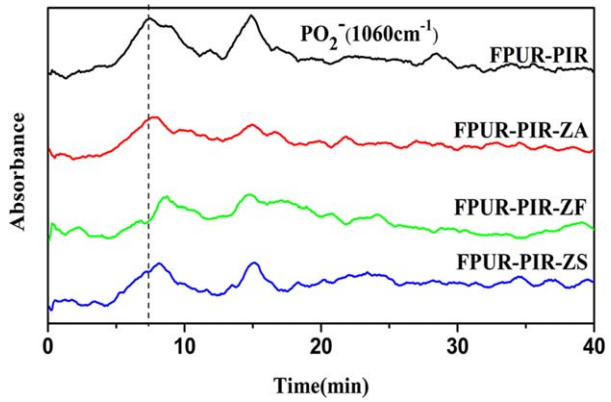

Figure 8. Relationship between intensity and released time for PO_2^-. [Color figure can be viewed in the online issue, which is available at wileyonlinelibrary.com.]

Smoke and Toxicity Mechanism

Two main mechanisms of smoke suppression in polymers with metal-containing compounds have been proposed: one is the Lewis acid mechanism[29] and the other is the reductive coupling mechanism.[30] However, the results of the two mechanisms are similar, in that metal salts promote the crosslinking of degradation fragments and char formation. In our work, we reduced

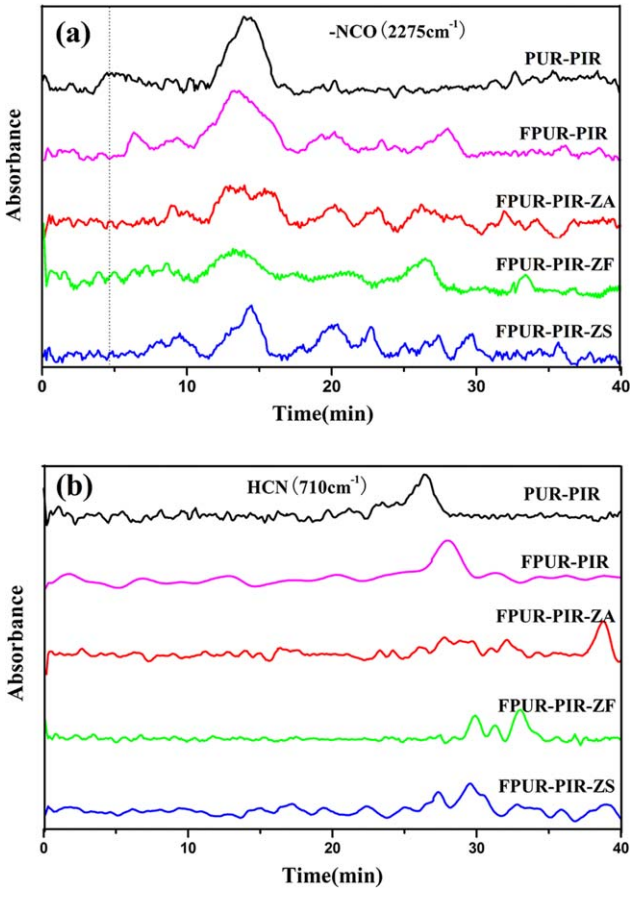

Figure 9. Relationship between intensity and released time for (a) –NCO and (b) HCN. [Color figure can be viewed in the online issue, which is available at wileyonlinelibrary.com.]

Table V. Ratio of Peaks Area per Unit of Mass Between FPUR-PIR and FPUR-PIR Filled with Zinc Salts

Evolved products	FPUR-PIR-ZA: FPUR-PIR (%)	FPUR-PIR-ZF: FPUR-PIR (%)	FPUR-PIR-ZS: FPUR-PIR (%)
PO_2^-	83.8	81.9	90.7
—NCO	63.6	82.7	88.2
HCN	68.5	63.7	75.0

the release of phosphorus oxides of phosphonate and chain scission of polymers following degradation. Combined with literature reports, the mechanisms of smoke and toxicity suppression by zinc salts in FPUR-PIR were analyzed as follows:

On the one hand, zinc salts delayed the release time of PO_2^-, this was due to zinc salts promoting the crosslinking between phosphorus oxide and polymer degradation products,[31] and inhibiting phosphorus oxide release into the gas phase. Coordination of the condensation of P—OH and P—O— groups with Me—OH surface groups and phosphoryl oxygen with surface Lewis acid sites are only some of the possible grafting configurations between organophosphorus groups and the polymer fragments[32] which promote crosslinking. Interactions between the phosphorus groups and degradation fragments of PUR-PIR are believed to promote char formation and inhibit the release of gas phase products from FPUR-PIR filled with zinc salts.

On the other hand, metal atoms in zinc salts may act as a Lewis acid and coordinate to the oxygen atom of the —NCO, causing the carbon of —NCO to be more electrophilic and more reactive with other molecular fragments. Generally speaking, these factors promote char formation and reduce the release of –NCO containing compounds.[33]

ZF is excellent for delaying the release time of PO_2^- which may be attributed to the fact than iron as a transition element has higher catalytic activity in char formation at the initial stage of thermal degradation.[15] In addition, ZA is excellent for delaying the release of HCN, possibly indicating that the stability of FPUR-PIR-ZA char, which delayed the release of nitrogen-

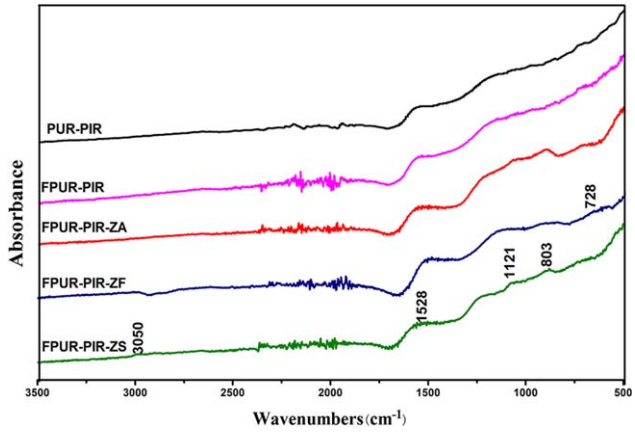

Figure 10. FTIR spectra of solid residues collected after CONE test. [Color figure can be viewed in the online issue, which is available at wileyonlinelibrary.com.]

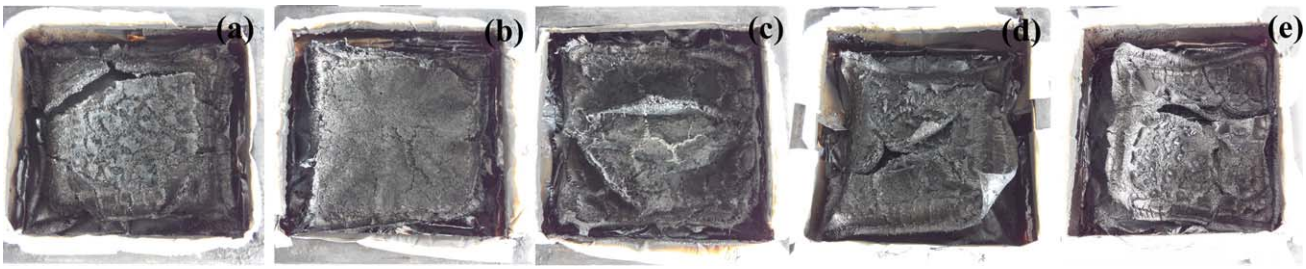

Figure 11. Digital photographs of residue char after the cone calorimeter test (a) PUR-PIR, (b) FPUR-PIR, FPUR-PIR filled with ZA (c), ZF (d), ZS (e). [Color figure can be viewed in the online issue, which is available at wileyonlinelibrary.com.]

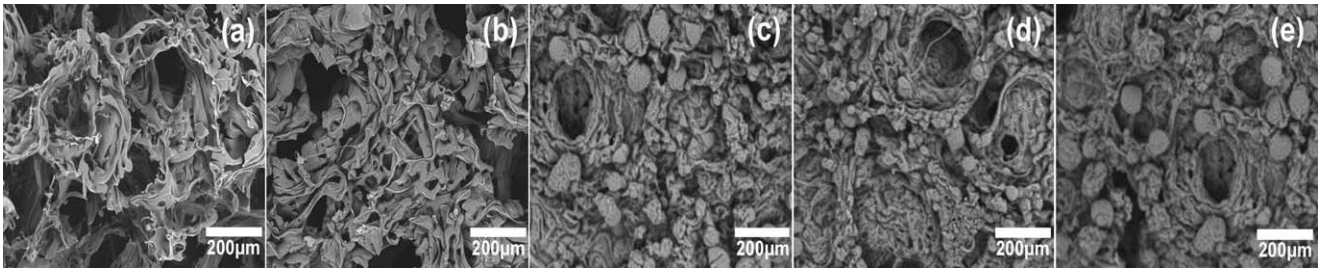

Figure 12. SEM micrograph of residue char after the cone calorimeter test (a) PUR-PIR, (b) FPUR-PIR, FPUR-PIR filled with ZA (c), ZF (d), ZS (e).

containing compounds at higher temperature, is better than other systems.

CONCLUSIONS

The aim of this study was to investigate the smoke and toxicity suppressive effects of zinc salt compounds on FPUR-PIR containing phosphonate and chlorinated phosphate as fire retardants. The degradation stages of FPUR-PIR were almost unchanged after the addition of zinc salts. Nevertheless, the SDR of FPUR-PIR filled with zinc salts was significantly reduced with no obvious change in LOI compared to FPUR-PIR. Zinc salts not only delayed the time to the second pk-HRR, but also increased the amount of char residue of FPUR-PIR in the CONE test.

The gas phase products of degradation were revealed by TG-FTIR. The initial release times of phosphorus oxide, isocyanate compounds and HCN were significantly delayed. This is because zinc salts weakened the gas phase effect of phosphorus and promoted char residue formation of FPUR-PIR. In addition, $ZnFe_2O_4$ performed better in char formation at the initial stage, and both FPUR-PIR and $ZnAl_2O_4$ retained more phosphorus in the solid phase at higher temperature.

In this study, zinc salts were found to suppress smoke and toxicity compounds related to FPUR-PIR-containing phosphonate and chlorinated phosphate fire retardants. The reasons for the different effects of the three types of zinc salts on smoke suppression are still not clear, and are the focus of our next study.

REFERENCES

1. Final Draft prEN 13501-1: Fire classification of construction products and building elements. Part 1: classification using testdata from reaction to fire tests.
2. Thirumal, M.; Khastgir, D.; Nando, G. B; Naik, Y. P.; Singha, N. K. *Polym. Degrad. Stab.* **2010**, *95*, 1138.
3. Anna, A. S.; Richard, H. T. *Energy Buildings* **2010**, *43*, 498.
4. Luis, A. F.; Miriam, G. A.; Leda, G.; Guido, M.; Manuel, A. G. *Forensic Sci. Int.* **2001**, *121*, 140.
5. Singh, H.; Jain, A. K. *J. App. Polym. Sci.* **2009**, *111*, 1115.
6. Checchin, M.; Cecchini, C.; Cellarosi, B.; Sam, F. O. *Polym. Degrad. Stab.* **1999**, *64*, 573.
7. Levin, B. C.; Braun, E.; Paabo, M.; Harris, R. H.; Navarro, M. *National Institute of Standards and Technology* **1992**, *36*, 38.
8. Chen, X. L.; Jiang, Y. F.; Jiao, C. M. *J. Hazard. Mater.* **2014**, *266*, 114.
9. Ning, Y.; Guo, S. *J. App. Polym. Sci.* **2000**, *77*, 3119.
10. Bauman, S. K. *J. Polym. Sci. Polym. Chem. Ed.* **1979**, *17*, 1129.
11. Dhakate, S. R; Mathur, R. B; Bahl, O. P. *Carbon* **1997**, *35*, 1753.
12. Weil, E. D.; Patel, N. G. *Polym. Degrad. Stab.* **2003**, *82*, 291.
13. Zhou, Y.; Hao, J. W.; Liu, G. S.; Du, J. X. *Chinese J. Inorgan. Chem.* **2013**, *29*, 1115.
14. Lin, M.; Li, B.; Li, Q. F.; Li, S.; Zhang, S. Q. *J. App. Polym. Sci.* **2011**, *121*,1951.
15. Gallo, E.; Schartel, B.; Acierno, D.; Russo, P. *Eur. Polym. J.* **2011**, *47*, 1390.
16. Wang, J. Q.; Li, B. *Polym. Degrad. Stab.* **1999**, *63*, 279.
17. Basfar, A. A. *Polym. Degrad. Stab.* **2003**, *82*, 333.
18. Horrocks, A. R.; Smart, G.; Kandola, B.; Holdsworth, A.; Price, D. *Polym. Degrad. Stab.* **2012**, *97*, 2503.
19. Su, X. Q.; Yi, Y. W.; Tao, J.; Qi, H. Q. *Polym. Degrad. Stab.* **2012**, *97*, 2108.

20. Matuschek, G. *Thermochimica Acta* **1995**, *263*, 59.
21. Wang, C. Q.; Ge, F. Y.; Sun, J.; Cai, Z. S. *J. App. Polym. Sci.* **2013**, *130*, 916.
22. Chen, X. L.; Jiao, C. M. *Polym. Degrad. Stab.* **2008**, *93*, 2222.
23. Hu, X. M.; Wang, D. M.; Wang, S. L. *Int. J. Mining Sci. Technol.* **2013**, *23*, 13.
24. Lorenzetti, A.; Modesti, M.; Besco, S.; Hrelja, D.; Donadi, S. *Polym. Degrad. Stab.* **2011**, *96*, 1455.
25. Jang, B. N.; Wilkie, C. A. *Thermochimica Acta* **2005**, *433*, 1.
26. Wang, H.; He, Q. S.; Mao, J. J.; Sun, Z. L.; J. H. *Procedia Eng.* **2013**, *52*, 377.
27. Chung, Y. J.; Kim, Y.; Kim, S. *J. Industrial Eng. Chem.* **2009**, *15*, 888.
28. Ramani, A.; Hagen, M.; Hereid, J.; Zhang, J. P.; Delichatsios, M. *Fire Mater.* **2010**, *34*, 77.
29. Edelson, D.; Kuck, V. J.; Lum, R. M. *Conbust. Flame.* **1980**, *38*, 271.
30. Lattimer, R. P.; Kroenke, W. J. *J. APP. Polym. Sci.* **1981**, *26*, 1191.
31. Duquesne, S.; Bras, M. L.; Delobel, R.; Camino, G.; Gengembre, L. *J. Fire Sci.* **2003**, *21*, 89.
32. Zhong, B.; Stanforth, R.; Wu, S.; Chen, J. P. *J. Colloid Interface Sci.* **2007**, *308*, 40.
33. Pengjam, W.; Saengfak, B. *J. App. Polym. Sci.* **2012**, *123*, 3520.